

# FEEDBACK CONTROL OF THE COVID-19 PANDEMIC WITH GUARANTEED NON-EXCEEDING ICU CAPACITY\*

THOMAS BERGER<sup>†</sup>

**Abstract.** In this paper we investigate feedback control techniques for the COVID-19 pandemic which are able to guarantee that the capacity of available intensive care unit beds is not exceeded. The control signal models the social distancing policies enacted by the local government. We propose a control design based on the bang-bang funnel controller which is robust with respect to uncertainties in the parameters of the epidemiological model and only requires measurements of the number of individuals who require medical attention. Therefore, it may serve as a first step towards a reliable decision making mechanism. Simulations illustrate the efficiency of the proposed controller.

**Key words.** COVID-19, adaptive control, funnel control, robust control, epidemiological models

**AMS subject classifications.** 37N25, 93C10, 93C40

**1. Introduction.** One of the most difficult problems in forecasting the effects of the COVID-19 pandemic is to generate reliable signals for policy makers in the presence of uncertain data and model parameters. To resolve this, in the present work a robust approach is taken, which is able to generate reliable signals for social distancing measures (or against them) in the presence of uncertainties in the parameters of the epidemiological model and which requires only measurements of the number of COVID-19 patients showing moderate to severe symptoms (and independent of possibly asymptomatic infected or patients with mild symptoms). The number of those symptomatic infected, who require medical attention, can typically be measured accurately – under the assumption that sufficient testing capabilities are available.

It is well documented [8, 12] that social distancing measures help to reduce infection rates and have an effect on the containment of the spread of SARS-CoV-2. On the other hand, social distancing has negative effects on both the economy and the mental and emotional health of the population. Therefore, policy makers face the hard decision of when to enact social distancing and when to relax the measures. The present paper may serve to provide a decision making mechanism based on a robust feedback control design.

In contrast to model-based techniques such as MPC (model-predictive control) used in [5, 9, 13] for instance, in the present paper we use a control methodology which does not require a specific model and is robust with respect to uncertainties in the system parameters. Because of the latter, it is not necessary to precisely identify all parameters such as the infection, recovery or death rates. Therefore, the approach may allow for an easier scalability, i.e., it may be applicable to different countries or regions or cities, without the need to precisely (re-)identify all the parameters for this region.

The above described question of when to enact social distancing measures or even a lockdown is a typical control theoretic question. Modelling this question utilizing a control input which takes only a finite number of different values, as suggested e.g. in [9], a suitable feedback controller is able to generate the required signals. In the present work we consider the simple case of a binary control input, i.e., with values in  $\{0, 1\}$ . To this end, we combine a widely used model for the description of the COVID-19 pandemic from [14] with a control component proposed in [13]. The latter adds additional dynamics to the model which account for the effects of social distancing policies represented by the value of the control input and the response of the population to them (paying heed to possible delays).

The control objective is to keep the number of infected with moderate to severe symp-

---

\*Preprint submitted to SIAM Journal on Control and Optimization, May 28, 2022

<sup>†</sup>Institut für Mathematik, Universität Paderborn, Warburger Str. 100, 33098 Paderborn, Germany  
(thomas.berger@math.upb.de).

toms (which typically require hospitalization) below a threshold defined by the number of available ICU (intensive care unit) beds. Another approach discussing control strategies which are able to bound the hospitalized population, by using control barrier functions, can be found in [1]. In the present paper, to achieve the control objective we exploit the bang-bang funnel controller developed in [11], which is able to guarantee error margins in tracking problems and the control input switches between only two values. Funnel control proved an appropriate tool in several applications such as temperature control of chemical reactor models [7], control of industrial servo-systems [6] and underactuated multibody systems [2], voltage and current control of electrical circuits [4], DC-link power flow control [15] and adaptive cruise control [3].

## 2. Epidemiological model for the COVID-19 pandemic and system class.

**2.1. Dynamics of the pandemic.** We use a so called SIRASD (Susceptible-Infected-Recovered-Asymptomatic-Symptomatic-Deceased) model for the dynamics of the COVID-19 pandemic from [13], which is able to account for possible social distancing policies. The resulting epidemiological model has the following dynamics:

$$\begin{aligned}
\dot{S}(t) &= -(\beta_A \psi(t) I_A(t) + \beta_S \psi(t) I_S(t)) \frac{S(t)}{N - D(t)}, \\
\dot{I}_A(t) &= (1 - p)(\beta_A \psi(t) I_A(t) + \beta_S \psi(t) I_S(t)) \frac{S(t)}{N - D(t)} - \alpha_A I_A(t), \\
(2.1) \quad \dot{I}_S(t) &= p(\beta_A \psi(t) I_A(t) + \beta_S \psi(t) I_S(t)) \frac{S(t)}{N - D(t)} - \frac{\alpha_S}{1 - \rho} I_S(t), \\
\dot{R}(t) &= \alpha_A I_A(t) + \alpha_S I_S(t), \\
\dot{D}(t) &= \frac{\rho \alpha_S}{1 - \rho} I_S(t), \\
\dot{\psi}(t) &= \gamma_0 (1 - \psi(t))(1 - u(t)) + \gamma_1 (K_\psi(t) \bar{\psi} - \psi(t)) u(t),
\end{aligned}$$

with the gain function

$$(2.2) \quad K_\psi(t) = 1 - \gamma_K \frac{\alpha_A \rho}{1 - \rho} \frac{I_A(t)}{N - D(t)}.$$

In (2.1) the total population of a considered region is split into the following compartments:

- susceptible individuals  $S(t)$ ,
- infected but asymptomatic individuals  $I_A(t)$ ,
- infected and symptomatic individuals  $I_S(t)$ ,
- recovered individuals  $R(t)$ ,
- deceased individuals  $D(t)$  (due to the disease).

It is easily seen that the derivative of the sum of the above quantities is zero,

$$\frac{d}{dt} (S(t) + I_A(t) + I_S(t) + R(t) + D(t)) = 0$$

for all  $t \geq 0$ , thus it stays constant over time and we may define the initial population (assuming  $D(0) = 0$ ) by

$$N := S(0) + I_A(0) + I_S(0) + R(0) = S(t) + I_A(t) + I_S(t) + R(t) + D(t), \quad t \geq 0.$$

The other parameters used in (2.1) are summarized in Table 2.1 and we emphasize that  $\alpha_A, \alpha_S, \beta_A, \beta_S, \rho, p, \gamma_0, \gamma_1, \bar{\psi} \in [0, 1]$ .

**2.2. Population response.** The last equation in (2.1) models the dynamics of social distancing policies and contains additional parameters to be explained in due course. The

Parameter	Epidemiological meaning
$\beta_A, \beta_S$	transmission coefficients (contact or infection rates) for an asymptomatic or symptomatic individual to transmit the disease to a susceptible individual, resp.
$\alpha_A, \alpha_S$	recovery rates for asymptomatic and symptomatic infected, resp.
$p$	proportion of individuals who develop symptoms
$\rho$	probability of a symptomatic infected individual to die from the disease before recovering
$\gamma_0, \gamma_1$	settling-time parameters used to determine the average time of the population response
$\bar{\psi}$	parameter which determines the strictest possible isolation
$\gamma_K$	positive gain coefficient

Table 2.1: Parameters of the SIRASD model (2.1).

simplest way to model the population response would be to replace the transmission coefficient  $\beta_x$ , where  $x$  stands for either  $A$  or  $S$ , by  $\beta_x(1 - u(t))$  as in [1], i.e., the control directly influences the infection rates. However, the population response is typically not instantaneous, but people change their behavior with a certain delay – this is accounted for by the last equation in (2.1). As introduced in [13], the function  $\psi$  can be seen as a time-varying population response which decreases the transmission coefficients  $\beta_A$  and  $\beta_S$  in the case that social distancing measures are in place. Possible delays in the response are modelled by the parameters  $\gamma_0, \gamma_1$ . Note that we have  $\psi(t) \in [0, 1]$  for all  $t \geq 0$ , where  $\psi(t) = 1$  stands for the case of no distancing at all and  $\psi(t) = 0$  would mean that any contacts between people are suppressed. Of course, the latter case is unachievable in practice, which is accounted for in the model. The control input  $u$  is assumed to take only binary values, i.e.,  $u(t) \in \{0, 1\}$  for all  $t \geq 0$ . This control signal models the policy enacted by the government, where  $u(t) = 0$  means that no isolation measures are in place, and  $u(t) = 1$  means that the government has determined social distancing.

The dynamics with which these measures influence the response of the population are modelled by the last equation in (2.1). Here, the value of the parameter  $\bar{\psi} \in (0, 1)$ , see Table 2.1, is additionally influenced by a gain function  $K_\psi$  defined in (2.2); the value of  $K_\psi(t)$  decreases as the proportion of asymptomatic infected individuals increases. Assuming that initially  $\psi(0) = 1$  (no isolation) we may infer that

$$(2.3) \quad \forall t \geq 0 : \psi(t) \in (\bar{K}_\psi \bar{\psi}, 1],$$

where  $\bar{K}_\psi = 1 - \gamma_K \frac{\alpha_A \rho}{1 - \rho}$ . For further details on the model (2.1) we refer to [13, 14].

**2.3. Control objective.** First note that, as in [13], we assume that the class of asymptomatic infected also includes those with only mild symptoms, which typically do not seek medical attention and are hence often not registered as infected. The class of symptomatic infected includes those with moderate to severe symptoms which may require ICU beds and are registered by local authorities – thus, provided that sufficient testing capabilities are available,  $I_S(t)$  is typically accurately measured.

The objective is to determine a control input signal  $u : \mathbb{R}_{\geq 0} \rightarrow \{0, 1\}$  which guarantees that the number of available ICU beds is not exceeded. This control signal may serve as an orientation for policy makers whether and when to enact social distancing measures. Since the class of symptomatic infected individuals encompasses those which may require ICU beds we seek to keep  $I_S(t)$  below the number  $n_{\text{ICU}}$  of available ICU beds, with tolerance  $\xi \geq 0$  accounting for symptomatic infected which do not require intensive care. In other

words, the aim is to achieve

$$(2.4) \quad \forall t \geq 0 : I_S(t) < (1 + \xi)n_{\text{ICU}}.$$

**2.4. System class.** We now turn to the specification of a class of systems described by the epidemiological model (2.1) amenable to the control strategy proposed in Section 3. The class of systems of the form (2.1) is defined by the set of admissible parameters

$$\Sigma := \left\{ (\alpha_A, \alpha_S, \beta_A, \beta_S, \rho, p, \gamma_0, \gamma_1, \bar{\psi}, \gamma_K, \xi, n_{\text{ICU}}, S^0, I_A^0, I_S^0, R^0, D^0, \psi^0) \in [0, 1]^9 \times [0, \infty)^9 \mid (\text{A1})-(\text{A3}) \text{ hold} \right\}$$

under the assumptions

$$(\text{A1}) \quad p > 0, \rho < 1, 0 < \alpha_S \leq \alpha_A \leq \frac{\alpha_S}{1-\rho}, \beta_S \leq \beta_A, p\beta_S \leq \frac{\alpha_S}{1-\rho} \text{ and } \beta_A \leq \gamma_1 + \alpha_A + \frac{\alpha_S}{1-\rho}$$

$$(\text{A2}) \quad S^0 > 0, R^0 > 0 \text{ and } I_A^0 \geq \frac{1-p}{p} I_S^0$$

$$(\text{A3}) \quad \varphi^+ > \frac{M_3}{2\zeta M_1} \text{ and } -\left(\frac{M_3}{\zeta M_1} + \varphi^+\right)\chi^2 + \frac{2\varphi^+ M_3}{\zeta M_1}\chi + \frac{3(p\beta_A N)^2}{2\zeta M_1} < 0, \text{ where}$$

$$(2.5) \quad \left\{ \begin{array}{l} \varphi^+ := (1 + \xi)n_{\text{ICU}}, \\ N := S^0 + I_A^0 + I_S^0 + R^0, \\ S_{\min}(S^0, R^0) := S^0 e^{-\frac{\beta_A(N-R^0)}{\alpha_S R^0}}, \\ \zeta := \frac{1}{p} \left( \gamma_1 + \alpha_A + \frac{(1-p\rho)\alpha_S}{1-\rho} + \beta_S \bar{K}_\psi \bar{\psi} \right), \\ M_1 := \frac{S_{\min}(S^0, R^0)}{N^2} \bar{K}_\psi \bar{\psi} \beta_S, \\ M_2 := \left( \frac{\alpha_S}{1-\rho} \right)^2, \\ M_3 := M_2 + \gamma_1 N M_1, \\ \chi := \frac{1}{3} \left( \frac{M_3}{\zeta M_1} + \varphi^+ \right) + \sqrt{\frac{1}{9} \left( \frac{M_3}{\zeta M_1} + \varphi^+ \right)^2 - \frac{\varphi^+ M_3}{3\zeta M_1}}. \end{array} \right.$$

We like to note that (A1) and (A2) are typically satisfied in real epidemiological scenarios, see also Section 5. The initial values  $S^0$  and  $R^0$  in (A2) for  $S(0) = S^0$  and  $R(0) = R^0$  are assumed to be positive to avoid technicalities and keep the proof of the main result simple. In fact, the assumption  $R(0) > 0$  is true for the COVID-19 pandemic in practically every country in the world and nearly every region by the date this article is written (and taken as  $t = 0$ ). Furthermore, in (A2) it is assumed that the initial values  $I_A(0) = I_A^0$  and  $I_S(0) = I_S^0$  satisfy  $I_A(0) \geq \frac{1-p}{p} I_S(0)$ , which is not a restrictive assumption since the number of asymptomatic infected is typically much larger than the number of symptomatic infected individuals; this is always satisfied, if  $I_S(0) = 0$ , which is typically the case at the beginning of a (local) outbreak. Finally, assumption (A3) is required to determine a non-empty range of control design parameters, see Section 3.

**3. Controller design.** In order to obtain a feedback control law which is able to guarantee the transient behavior in (2.4) (and hence to achieve the control objective), we exploit the idea of bang-bang funnel control from [11]. “Bang-bang” means that the control input switches between only two different values, hence this technique is suitable for our purposes. We stress that system (2.1) does not belong to the class of systems investigated in [11] and hence feasibility of bang-bang funnel control needs to be investigated separately. However, due to the special structure of (2.1) a simpler control law is possible here. To be

precise, we consider the controller

$$(3.1) \quad u(t) = \begin{cases} 1, & \text{if } I_S(t) \geq \varphi^+ - \varepsilon^+, \\ 0, & \text{if } I_S(t) \leq \varphi^- + \varepsilon^-, \\ u(t-), & \text{otherwise,} \end{cases}$$

where  $\varphi^+, \varphi^-, \varepsilon^+, \varepsilon^-$  are non-negative parameters satisfying  $\varphi^- + \varepsilon^- < \varphi^+ - \varepsilon^+$  and by  $u(t-)$  we denote the left limit  $u(t-) = \lim_{h \searrow 0} u(t-h)$  of the piecewise constant function  $u$  at  $t$ . The controller is initialized by  $u(0-) = 0$ .

In [11]  $\varphi^+$  and  $\varphi^-$  are time-varying functions which determine a performance funnel for a certain signal to evolve in and  $\varepsilon^+, \varepsilon^-$  are “safety distances” required to guarantee that the signal evolves within this funnel. In the present paper, the aim is to achieve  $I_S(t) \in [\varphi^-, \varphi^+]$ , thus, in view of the control objective formulated in Subsection 2.3, we may choose

$$(3.2) \quad \varphi^- := 0, \quad \varphi^+ := (1 + \xi)n_{\text{ICU}}.$$

We emphasize that the feedback control strategy (3.1) only requires the measurement of the number  $I_S(t)$  of symptomatic infected individuals at time  $t$ , which, as mentioned in Section 2, can be measured accurately.

In the following we identify conditions on the “safety distances”  $\varepsilon^+, \varepsilon^-$  so that the application of the controller (3.1) to a system (2.1) with a tuple of parameters from  $\Sigma$  is feasible. In essence, these assumptions mean that by maintaining a strict lockdown, i.e.,  $u(t) = 1$  for  $t \geq 0$ , it is possible to guarantee (2.4). If this is not possible, then no switching strategy can be successful.

The pairs of feasible control parameters depend on the choice of system parameters in general. For any  $Z \in \Sigma$  we define the control parameter set

$$C_Z := \{ (\varepsilon^-, \varepsilon^+) \in (0, \infty)^2 \mid (\text{A4})-(\text{A5}) \text{ hold } \},$$

under the assumptions, where we use the constants defined in (2.5) in terms of  $Z$ ,

$$(\text{A4}) \quad \varepsilon^- > \chi,$$

$$(\text{A5}) \quad \frac{(p\beta_A N)^2}{2\varepsilon^-(\zeta M_1 \varepsilon^- - M_3)} < \varepsilon^+ < \varphi^+ - \varepsilon^-.$$

Assumptions (A4) and (A5) are quite conservative since they are designed for worst-case scenarios, and hence they may impose hard restrictions in practice. However, the controller (3.1) may even be feasible if these assumptions are not satisfied and appropriate values for  $\varepsilon^+$  and  $\varepsilon^-$  can be identified by simulations.

It can be seen that, while (A4) simply gives a lower bound for  $\varepsilon^-$ , assumption (A5) requires  $\varepsilon^+$  to be within a range, where both the lower and upper bound depend on  $\varepsilon^-$ . Therefore, the question arises whether (A4) and (A5) can be simultaneously satisfied. The following result gives an affirmative answer to this question, which is based on the assumptions (A1)–(A3) on the system parameters  $Z$ .

LEMMA 3.1. *For all  $Z \in \Sigma$  the set  $C_Z$  is non-empty and open.*

*Proof.* We show that there exist  $\varepsilon^-, \varepsilon^+ > 0$  which satisfy (A4) and (A5). This is true if, and only if, there exists  $\varepsilon^- > \chi$  which satisfies

$$(3.3) \quad \frac{(p\beta_A N)^2}{2\varepsilon^-(\zeta M_1 \varepsilon^- - M_3)} < \varphi^+ - \varepsilon^-.$$

First we show that the expression on the left hand side is well defined, i.e., that  $\zeta M_1 \varepsilon^- - M_3 > 0$ . This follows by invoking that (A3) gives  $\varphi^+ > \frac{M_3}{2\zeta M_1}$  and hence we have

$$\varepsilon^- > \chi > \frac{2}{3} \left( \frac{M_3}{\zeta M_1} + \varphi^+ \right) > \frac{M_3}{\zeta M_1}.$$

Condition (3.3) is equivalent to

$$0 > 2\varepsilon^-(\varepsilon^- - \varphi^+)(\zeta M_1 \varepsilon^- - M_3) + (p\beta_A N)^2 = q(\varepsilon^-)$$

for the polynomial  $q(s) = 2\zeta M_1 s^3 - 2(\zeta M_1 \varphi^+ + M_3)s^2 + 2M_3 \varphi^+ s + (p\beta_A N)^2$ . It is straightforward to verify that  $q'(\chi) = 0$  and  $q''(\chi) > 0$  for  $\chi$  as in (2.5), hence  $\chi$  is a (positive) local minimum of  $q(s)$ . Furthermore, we find that

$$\chi^2 - \left( \frac{M_3}{\zeta M_1} + \varphi^+ \right) \chi + \frac{\varphi^+ M_3}{\zeta M_1} = -\frac{1}{3} \left( \frac{M_3}{\zeta M_1} + \varphi^+ \right) \chi + \frac{2\varphi^+ M_3}{3\zeta M_1},$$

hence, by (A3),

$$\begin{aligned} 0 &> - \left( \frac{M_3}{\zeta M_1} + \varphi^+ \right) \chi^2 + \frac{2\varphi^+ M_3}{\zeta M_1} \chi + \frac{3(p\beta_A N)^2}{2\zeta M_1} \\ &= 3 \left( \chi^3 - \left( \frac{M_3}{\zeta M_1} + \varphi^+ \right) \chi^2 + \frac{\varphi^+ M_3}{\zeta M_1} \chi \right) + \frac{3(p\beta_A N)^2}{2\zeta M_1} = \frac{3}{2\zeta M_1} q(\chi). \end{aligned}$$

Then  $q(\chi) < 0$  yields that there exists  $\varepsilon^- > \chi$  such that  $q(\varepsilon^-) < 0$ , which shows that the set  $C_Z$  is non-empty. Finally, from assumptions (A4) and (A5) it is clear that  $C_Z$  is open.  $\square$

#### 4. Main results.

**4.1. Feasibility of the control design.** In the following first main result of the present paper we prove that, for any tuple of system parameters  $Z \in \Sigma$  and any pair of controller parameters  $(\varepsilon^-, \varepsilon^+) \in C_Z$ , the application of the bang-bang control law (3.1) with parameters  $(\varepsilon^-, \varepsilon^+)$  to the epidemiological model (2.1) with parameters  $Z$  leads to a closed-loop system, which has a global and bounded solution that satisfies (2.4). Moreover, the control input  $u$  has only a finite number of jumps in each compact set. Solutions are considered in the sense of Carathéodory, i.e., they are assumed to be locally absolutely continuous and satisfy the differential equation almost everywhere. A solution is said to be maximal, if it has no right extension that is also a solution.

**THEOREM 4.1.** *Let  $Z \in \Sigma$  and consider the associated system (2.1). Further let  $(\varepsilon^-, \varepsilon^+) \in C_Z$  be a pair of controller parameters,  $\varphi^+$  be as in (3.2) and assume that*

$$I_S^0 \in [0, \varphi^+ - \varepsilon^+], \quad D^0 = 0 \quad \text{and} \quad \psi^0 = 1.$$

*Then the controller (3.1) applied to (2.1) leads to a closed-loop system which has a global and bounded solution  $(S, I_A, I_S, R, D, \psi) : \mathbb{R}_{\geq 0} \rightarrow (\mathbb{R}_{\geq 0})^6$  such that  $\dot{I}_S$  is bounded, (2.4) holds and  $u$  defined by (3.1) has locally finitely many jumps.*

*Proof.* Throughout the proof we use the constants defined in (2.5) without further notice. We divide the proof into several steps.

*Step 1:* We show the existence of a local solution. In fact, repeating the arguments of [10, Cor. 3.3] or [11, Thm. 5.3] yields a maximal solution  $(S, I_A, I_S, R, D, \psi) : [0, \omega) \rightarrow \mathbb{R}^6$  of (2.1), (3.1) with  $\omega \in (0, \infty]$ . Note that clearly the solution is bounded as each component is non-negative and we have  $S(t) + I_A(t) + I_S(t) + R(t) + D(t) = N$  and  $\psi(t) \leq 1$  for all  $t \in [0, \omega)$ . Therefore, we have that  $N - D(t) = S(t) + I_A(t) + I_S(t) + R(t) \geq S(t)$  by which  $\frac{S(t)}{N - D(t)} \leq 1$  for all  $t \in [0, \omega)$  and hence the respective quotient in (2.1) is uniformly bounded.

*Step 2:* We show that  $\dot{I}_S$  is bounded on  $[0, \omega)$ . This is a consequence of (2.3) and Step 1, by which

$$\dot{I}_S(t) \leq p(\beta_A I_A(t) + \beta_S I_S(t)) - \frac{\alpha_S}{1 - \rho} I_S(t) \leq p\beta_A N + \left( p\beta_S - \frac{\alpha_S}{1 - \rho} \right) I_S(t) \stackrel{(A1)}{\leq} p\beta_A N$$

for all  $t \in [0, \omega)$ .

*Step 3:* We show that  $u$  has only finitely many jumps in each interval  $[a, b) \subseteq [0, \omega)$ . Seeking a contradiction assume that there exists an interval containing infinitely many jumps. Then there exist sequences  $(t_n), (s_n) \subseteq [a, b)$  with  $t_n < s_n < t_{n+1}$  for all  $n \in \mathbb{N}$  and, without loss of generality,  $t_n \rightarrow b$  for  $n \rightarrow \infty$  (otherwise we choose a smaller interval) such that  $u(t) = 1$  for all  $t \in [t_n, s_n)$  and  $u(t) = 0$  for all  $t \in [s_n, t_{n+1})$  and all  $n \in \mathbb{N}$ . Then (3.1) implies that  $I_S(t_n) = \varphi^+ - \varepsilon^+ > \varepsilon^- = I_S(s_n)$ . Therefore, by the mean value theorem there exists  $\lambda_n \in (t_n, s_n)$  such that

$$\dot{I}_S(\lambda_n) = \frac{I_S(t_n) - I_S(s_n)}{t_n - s_n} = \frac{\varphi^+ - \varepsilon^+ - \varepsilon^-}{t_n - s_n} \rightarrow \infty \quad \text{as } n \rightarrow \infty,$$

which contradicts boundedness of  $\dot{I}_S$  from Step 2.

*Step 4:* We show that  $\omega = \infty$ . Since  $(S, I_A, I_S, R, D, \psi)$  is bounded as  $S(t) + I_A(t) + I_S(t) + R(t) + D(t) = N$  and  $\psi(t) \leq 1$  for all  $t \in [0, \omega)$ , the case  $\omega < \infty$  is only possible when the jumps in  $u$  accumulate for  $t \rightarrow \omega$ , but this is excluded by Step 3.

*Step 5:* We show that  $I_A(t) \geq \frac{1-p}{p} I_S(t)$  for all  $t \geq 0$ . To this end, set  $z(t) := I_A(t) - \frac{1-p}{p} I_S(t)$  for  $t \geq 0$ . Then

$$\dot{z}(t) = -\alpha_A I_A(t) + \frac{1-p}{p} \frac{\alpha_S}{1-\rho} I_S(t) = -\alpha_A z(t) + \frac{1-p}{p} \left( \frac{\alpha_S}{1-\rho} - \alpha_A \right) I_S(t) \stackrel{(A1)}{\geq} -\alpha_A z(t)$$

for all  $t \geq 0$ , and hence Grönwall's lemma implies  $z(t) \geq e^{-\alpha_A t} z(0)$ . Therefore, we have  $I_A(t) \geq e^{-\alpha_A t} z(0) + \frac{1-p}{p} I_S(t) \geq \frac{1-p}{p} I_S(t)$ , where the last inequality follows from the assumption  $I_A(0) \geq \frac{1-p}{p} I_S(0)$  in (A2).

*Step 6:* We show that  $S(t) \geq S_{\min}(S^0, R^0)$  for all  $t \geq 0$ , where  $S_{\min}(S^0, R^0)$  is as defined in (A3). We find that, invoking  $N - D(t) \geq R(t) \geq R^0$ ,

$$\begin{aligned} \dot{S}(t) &= -(\beta_A \psi(t) I_A(t) + \beta_S \psi(t) I_S(t)) \frac{S(t)}{N - D(t)} \stackrel{(2.3)}{\geq} -(\beta_A I_A(t) + \beta_S I_S(t)) \frac{S(t)}{R^0} \\ &\stackrel{(A1)}{\geq} -\beta_A \left( \frac{\alpha_A}{\alpha_A} I_A(t) + \frac{\alpha_S}{\alpha_S} I_S(t) \right) \frac{S(t)}{R^0} \stackrel{(A1)}{\geq} -\frac{\beta_A}{\alpha_S} (\alpha_A I_A(t) + \alpha_S I_S(t)) \frac{S(t)}{R^0} \\ &= -\frac{\beta_A}{\alpha_S} \frac{\dot{R}(t)}{R^0} S(t) \end{aligned}$$

for all  $t \geq 0$ . Then Grönwall's lemma implies that, for all  $t \geq 0$ ,

$$S(t) \geq S^0 \exp \left( -\frac{\beta_A}{\alpha_S} \int_0^t \frac{\dot{R}(s)}{R^0} ds \right) = S^0 e^{-\frac{\beta_A (R(t) - R^0)}{\alpha_S R^0}} \geq S^0 e^{-\frac{\beta_A (N - R^0)}{\alpha_S R^0}} = S_{\min}(S^0, R^0).$$

*Step 7:* It remains to show (2.4). To this end, let  $t_0 \geq 0$  be such that  $I_S(t_0) = \varphi^+ - \varepsilon^+$  and

$$t_1 := \inf \{ t \geq t_0 \mid I_S(t) = \varepsilon^- \},$$

where  $t_1 = \infty$  is possible, if the above set is empty. We show that  $I_S(t) \leq \varphi^+$  for all  $t \in [t_0, t_1)$ , which in view of  $I_S(0) \leq \varphi^+ - \varepsilon^+$  proves the claim.

First, we show that  $\ddot{I}_S(t) \leq -M \varepsilon^-$  for all  $t \in [t_0, t_1)$  for  $M := \zeta M_1 \varepsilon^- - M_3$ . Since  $\varepsilon^- \stackrel{(A4)}{>} \chi \stackrel{(A3)}{>} \frac{M_3}{\zeta M_1}$ , we have that  $M > 0$ . Observe that by (3.1) we have  $u(t) = 1$  for all

$t \in [t_0, t_1]$  and hence  $\dot{\psi}(t) = \gamma_1(K_\psi(t)\bar{\psi} - \psi(t)) < 0$ . Furthermore, we calculate

$$\begin{aligned}
\ddot{I}_S(t) &= p\dot{\psi}(t)(\beta_A I_A(t) + \beta_S I_S(t)) \frac{S(t)}{N - D(t)} + p\psi(t)(\beta_A \dot{I}_A(t) + \beta_S \dot{I}_S(t)) \frac{S(t)}{N - D(t)} \\
&\quad + p\psi(t)(\beta_A I_A(t) + \beta_S I_S(t)) \frac{\dot{S}(t)(N - D(t)) + S(t)\dot{D}(t)}{(N - D(t))^2} - \frac{\alpha_S}{1 - \rho} \dot{I}_S(t) \\
&\stackrel{(2.1)}{\leq} p\gamma_1 K_\psi(t)\bar{\psi}(\beta_A I_A(t) + \beta_S I_S(t)) \frac{S(t)}{N - D(t)} + p\gamma_1 \dot{S}(t) \\
&\quad - p\psi(t)\left(\beta_A((1 - p)\dot{S}(t) + \alpha_A I_A(t)) + \beta_S(p\dot{S}(t) + \frac{\alpha_S}{1 - \rho} I_S(t))\right) \frac{S(t)}{N - D(t)} \\
&\quad + p\psi(t)(\beta_A I_A(t) + \beta_S I_S(t)) \frac{\dot{S}(t)}{N - D(t)} - \frac{p\rho\alpha_S}{1 - \rho} \frac{\dot{S}(t)I_S(t)}{N - D(t)} \\
&\quad + \frac{\alpha_S}{1 - \rho} \left(p\dot{S}(t) + \frac{\alpha_S}{1 - \rho} I_S(t)\right) \\
&= p\gamma_1 K_\psi(t)\bar{\psi}(\beta_A I_A(t) + \beta_S I_S(t)) \frac{S(t)}{N - D(t)} \\
&\quad + \left(\frac{\alpha_S}{1 - \rho}\right)^2 I_S(t) - p\psi(t)\left(\alpha_A \beta_A I_A(t) + \frac{\alpha_S \beta_S}{1 - \rho} I_S(t)\right) \frac{S(t)}{N - D(t)} \\
&\quad + p\dot{S}(t)\left(\gamma_1 + \frac{\alpha_S}{1 - \rho} - \psi(t)(\beta_A(1 - p) + p\beta_S)\frac{S(t)}{N - D(t)}\right. \\
&\quad \left. + (\beta_A I_A(t) + \beta_S I_S(t))\frac{\psi(t)}{N - D(t)} - \frac{\rho\alpha_S}{1 - \rho} \frac{I_S(t)}{N - D(t)}\right) \\
&\stackrel{(A1)}{\leq} p\gamma_1 K_\psi(t)\bar{\psi}(\beta_A I_A(t) + \beta_S I_S(t)) \frac{S(t)}{N - D(t)} + \left(\frac{\alpha_S}{1 - \rho}\right)^2 I_S(t) \\
&\quad + p\frac{\dot{S}(t)}{N - D(t)} \left(\left(\gamma_1 + \alpha_A + \frac{\alpha_S}{1 - \rho}\right)(N - D(t))\right. \\
&\quad \left. - \psi(t)(\beta_A(1 - p) + p\beta_S)S(t) + (\beta_A I_A(t) + \beta_S I_S(t))\psi(t) - \frac{\rho\alpha_S}{1 - \rho} I_S(t)\right)
\end{aligned}$$

for all  $t \in [t_0, t_1]$ . Next we aim to estimate the last term in the brackets above, that is

$$\begin{aligned}
&\left(\gamma_1 + \alpha_A + \frac{\alpha_S}{1 - \rho}\right)(N - D(t)) - \psi(t)(\beta_A(1 - p) + p\beta_S)S(t) + (\beta_A I_A(t) + \beta_S I_S(t))\psi(t) \\
&- \frac{\rho\alpha_S}{1 - \rho} I_S(t) \\
&\stackrel{(2.3), (A1)}{\geq} \left(\gamma_1 + \alpha_A + \frac{\alpha_S}{1 - \rho}\right)(N - D(t)) - \beta_A S(t) + (\beta_A I_A(t) + \beta_S I_S(t))\bar{K}_\psi \bar{\psi} - \frac{\rho\alpha_S}{1 - \rho} I_S(t) \\
&\geq \left(\gamma_1 + \alpha_A + \frac{\alpha_S}{1 - \rho}\right)(S(t) + I_A(t) + I_S(t)) - \beta_A S(t) + (\beta_A I_A(t) + \beta_S I_S(t))\bar{K}_\psi \bar{\psi} \\
&- \frac{\rho\alpha_S}{1 - \rho} I_S(t) \\
&= \left(\gamma_1 + \alpha_A + \frac{\alpha_S}{1 - \rho} - \beta_A\right) S(t) + \left(\gamma_1 + \alpha_A + \frac{\alpha_S}{1 - \rho} + \beta_A \bar{K}_\psi \bar{\psi}\right) I_A(t) \\
&\quad + \left(\gamma_1 + \alpha_A + \frac{\alpha_S}{1 - \rho} + \beta_S \bar{K}_\psi \bar{\psi} - \frac{\rho\alpha_S}{1 - \rho}\right) I_S(t) \\
&\stackrel{\text{Step 5, (A1)}}{\geq} \left(\gamma_1 + \alpha_A + \frac{\alpha_S}{1 - \rho} - \beta_A\right) S(t) + \frac{1}{p} \left(\gamma_1 + \alpha_A + \frac{(1 - p\rho)\alpha_S}{1 - \rho} + \beta_S \bar{K}_\psi \bar{\psi}\right) I_S(t) =: (*).
\end{aligned}$$

Invoking the last condition in (A1) and the fact that  $I_S(t) > \varepsilon^-$  for all  $t \in [t_0, t_1]$  we may further estimate the above term by

$$(*) > \frac{1}{p} \left( \gamma_1 + \alpha_A + \frac{(1-p\rho)\alpha_S}{1-\rho} + \beta_S \bar{K}_\psi \bar{\psi} \right) \varepsilon^- = \zeta \varepsilon^-.$$

With this we find that, invoking  $\psi(t) > K_\psi(t)\bar{\psi}$ ,

$$\begin{aligned} \ddot{I}_S(t) &< p\gamma_1 K_\psi(t)\bar{\psi}(\beta_A I_A(t) + \beta_S I_S(t)) \frac{S(t)}{N-D(t)} + \left( \frac{\alpha_S}{1-\rho} \right)^2 I_S(t) + p\zeta \varepsilon^- \frac{\dot{S}(t)}{N-D(t)} \\ &= p(\beta_A I_A(t) + \beta_S I_S(t)) \frac{S(t)}{(N-D(t))^2} (\gamma_1 K_\psi(t)\bar{\psi}(N-D(t)) - \zeta \varepsilon^- \psi(t)) + \left( \frac{\alpha_S}{1-\rho} \right)^2 I_S(t) \\ &\leq p(\beta_A I_A(t) + \beta_S I_S(t)) \frac{S(t)}{(N-D(t))^2} K_\psi(t)\bar{\psi}(\gamma_1 N - \zeta \varepsilon^-) + \left( \frac{\alpha_S}{1-\rho} \right)^2 I_S(t) \\ &\stackrel{(**)}{\leq} \beta_S I_S(t) \frac{S(t)}{N^2} \bar{K}_\psi \bar{\psi}(\gamma_1 N - \zeta \varepsilon^-) + \left( \frac{\alpha_S}{1-\rho} \right)^2 I_S(t) \\ &\stackrel{\text{Step 6}}{\leq} \left( \frac{S_{\min}(S^0, R^0)}{N^2} \bar{K}_\psi \bar{\psi} \beta_S (\gamma_1 N - \zeta \varepsilon^-) + \left( \frac{\alpha_S}{1-\rho} \right)^2 \right) I_S(t) = -M I_S(t) \leq -M \varepsilon^- \end{aligned}$$

for all  $t \in [t_0, t_1]$ , where  $\varepsilon^- > 0$  by (A4) and  $(**)$  follows from Step 5, (A1) and the observation that since  $M > 0$  we have

$$\zeta \varepsilon^- > \frac{M_3}{M_1} = \gamma_1 N + \frac{M_2}{M_1} > \gamma_1 N.$$

Upon integration we obtain that  $\dot{I}_S(t) = \dot{I}_S(t_0) + \int_{t_0}^t \ddot{I}_S(s) ds < \dot{I}_S(t_0) - M \varepsilon^- (t - t_0)$  for  $t \in [t_0, t_1]$  and a second integration gives

$$\begin{aligned} I_S(t) &< I_S(t_0) + \dot{I}_S(t_0)(t - t_0) - \frac{1}{2} M \varepsilon^- (t - t_0)^2 \\ &\stackrel{\text{Step 2}}{\leq} \varphi^+ - \varepsilon^+ + p\beta_A N(t - t_0) - \frac{1}{2} M \varepsilon^- (t - t_0)^2. \end{aligned}$$

Define the polynomial  $q(t) := -\varepsilon^+ + p\beta_A N(t - t_0) - \frac{1}{2} M \varepsilon^- (t - t_0)^2$  and observe that it attains its maximum at  $\tau = t_0 + \frac{p\beta_A N}{M \varepsilon^-}$ , hence

$$I_S(t) < \varphi^+ + q(\tau) = \varphi^+ - \varepsilon^+ + \frac{(p\beta_A N)^2}{2M\varepsilon^-} \stackrel{(\text{A5})}{<} \varphi^+$$

for all  $t \in [t_0, t_1]$ . This finishes the proof of the theorem.  $\square$

We like to note that in Theorem 4.1 it is assumed that the initial value  $I_S(0)$  lies within a certain interval. If the upper bound  $I_S(0) \leq \varphi^+ - \varepsilon^+$  does not hold, then even a hard lockdown with  $u(t) = 1$  for  $t \geq 0$  may not be sufficient to guarantee (2.4).

**4.2. Robustness of the control design.** In the following second main result we show that, when the controller parameters  $(\varepsilon^-, \varepsilon^+)$  are fixed, then there exists an open subset of the set  $\Sigma$  of admissible system parameters, so that the controller (3.1) with  $(\varepsilon^-, \varepsilon^+)$  is feasible for every system (2.1) with parameters from this open set. In other words, the controller (3.1) is robust with respect to uncertainties in the system parameters. Since the feasibility of (3.1) follows from Theorem 4.1, it is sufficient to show that  $(\varepsilon^-, \varepsilon^+) \in C_Z$  is contained in any set  $C_{\tilde{Z}}$  for  $\tilde{Z}$  in a neighborhood of  $Z$ .

**THEOREM 4.2.** *For all interior points  $Z$  of  $\Sigma$  and all  $(\varepsilon^-, \varepsilon^+) \in C_Z$  there exists  $\delta > 0$  such that  $B_\delta(Z) \subseteq \Sigma$  and*

$$\forall \tilde{Z} \in B_\delta(Z) : (\varepsilon^-, \varepsilon^+) \in C_{\tilde{Z}},$$

where  $B_\delta(Z)$  denotes the open ball with radius  $\delta$  around  $Z$  in  $[0, 1]^9 \times [0, \infty)^9$ .

*Proof.* Let  $Z \in \Sigma$  and  $(\varepsilon^-, \varepsilon^+) \in C_Z$  be fixed. Since  $Z$  is an interior point of  $\Sigma$  there exists  $\delta_1 > 0$  such that  $B_{\delta_1}(Z) \subseteq \Sigma$ . For any  $\tilde{Z} \in \Sigma$  consider the polynomial  $q(s) = q_{\tilde{Z}}(s)$  defined in the proof of Lemma 3.1 and recall that  $q_{\tilde{Z}}(\chi) < 0$ , where  $\chi = \chi(\tilde{Z})$  is as in (2.5). Furthermore, by the definition of  $q(s)$ , it has exactly one zero larger than  $\chi$ , denoted by  $\lambda^+ = \lambda^+(\tilde{Z})$ , and clearly  $q(s) < 0$  for all  $\chi < s < \lambda^+$ . Moreover, a careful inspection of the proof of Lemma 3.1 reveals that (3.3) is satisfied with  $\varepsilon^- = s$  for all  $\chi < s < \lambda^+$ . Therefore, with the functions

$$\begin{aligned} f_1 : B_{\delta_1}(Z) &\rightarrow \mathbb{R}, \quad \tilde{Z} \mapsto \chi, \quad f_2 : B_{\delta_1}(Z) \rightarrow \mathbb{R}, \quad \tilde{Z} \mapsto \lambda^+, \\ f_3 : \left\{ (\tilde{Z}, s) \in B_{\delta_1}(Z) \times \mathbb{R} \mid s > \frac{M_3}{\zeta M_1} \right\} &\rightarrow \mathbb{R}, \quad (\tilde{Z}, s) \mapsto \frac{(p\beta_A N)^2}{2s(\zeta M_1 s - M_3)}, \\ f_4 : B_{\delta_1}(Z) \times \mathbb{R} &\rightarrow \mathbb{R}, \quad (\tilde{Z}, s) \mapsto \varphi^+ - s, \end{aligned}$$

we find that, for all  $\tilde{Z} \in B_{\delta_1}(Z)$ ,

$$C_{\tilde{Z}} = \left\{ (s, t) \in (0, \infty)^2 \mid s \in (f_1(\tilde{Z}), f_2(\tilde{Z})), t \in (f_3(\tilde{Z}, s), f_4(\tilde{Z}, s)) \right\}.$$

Now we have that

$$\varepsilon^- \in (f_1(Z), f_2(Z)), \quad \varepsilon^+ \in (f_3(Z, \varepsilon^-), f_4(Z, \varepsilon^-)),$$

and since  $f_1, f_2$  are continuous and  $\tilde{Z} \mapsto f_i(\tilde{Z}, \varepsilon^-)$  is continuous as well on  $B_{\delta_1}(Z)$  for  $i = 3, 4$ , there exists  $\delta \in (0, \delta_1)$  such that

$$\forall \tilde{Z} \in B_{\delta}(Z) : \varepsilon^- \in (f_1(\tilde{Z}), f_2(\tilde{Z})), \quad \varepsilon^+ \in (f_3(\tilde{Z}, \varepsilon^-), f_4(\tilde{Z}, \varepsilon^-)),$$

which finishes the proof.  $\square$

While we have shown in Theorem 4.2 that, for a fixed pair of controller parameters, the control strategy (3.1) is robust with respect to uncertainties in the system parameters, it still depends on the structure of the model (2.1). Nevertheless, if a different epidemiological model is chosen, replacing (2.1), then by Theorem 4.1, *mutatis mutandis*, the controller (3.1) is still feasible for a suitable choice of parameters  $(\varepsilon^-, \varepsilon^+)$  and its robustness properties are retained.

**5. Simulations.** In this section we illustrate our findings by a simulation of the epidemiological model (2.1) under the feedback control law (3.1). We emphasize that it is not the purpose of the present paper to model the COVID-19 pandemic for a specific region, but to demonstrate that a funnel control approach achieves robustness with respect to uncertainties in the system parameters.

For the simulation we consider a population of  $N = 10^5$  individuals in an *Example City*. At time  $t = 0$  the population of *Example City* is divided into

$$S(0) = 0.85 \cdot 10^5 - 10, \quad I_A(0) = 10, \quad I_S(0) = 0, \quad R(0) = 0.15 \cdot 10^5, \quad D(0) = 0,$$

i.e., we have ten asymptomatic infected, who, for instance, caught the disease during a stay in another region. Furthermore, we assume that 15% of the population already developed immunity due to a prior disease and hence belong to the class of recovered individuals. This number may be reasonable for the COVID-19 pandemic (at least in some regions in Germany) as e.g. the COVID-19 Case-Cluster-Study [16] (Heinsberg study) suggests.

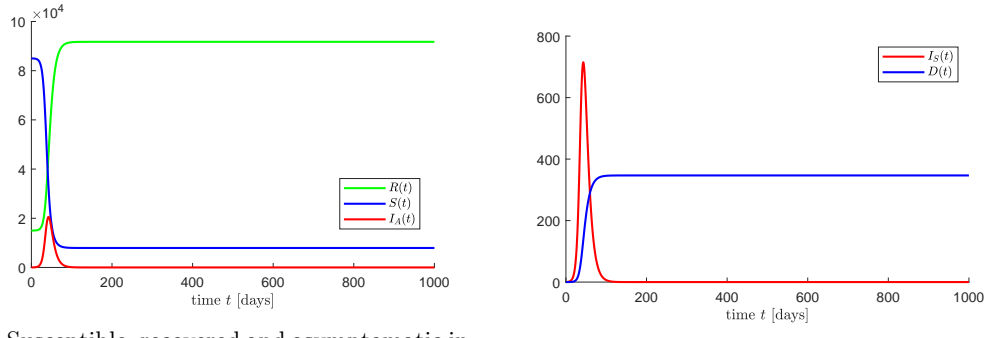
We further assume that the disease spreads in *Example City* according to the parameters that have been used in [13] and which are summarized in Table 5.1.

The number of available ICU beds in *Example City* is assumed to correspond to the available capacity in Germany, which are 32637 beds (based on data from [de.statista.com](http://de.statista.com),

$\beta_A$	$\beta_S$	$\alpha_A$	$\alpha_S$	$p$	$\rho$	$\gamma_0$	$\gamma_1$	$\bar{\psi}$	$\gamma_K$
0.43	0.37	0.14	0.1	0.03	0.15	1	1	0.35	1

Table 5.1: Parameter values for the SIRASD model (2.1) taken from [13, Sec. 3.2] for the case of the “Uncertain 2” model.

July 21, 2020) for a population of about  $8.3 \cdot 10^7$ . Preserving this ratio, we obtain for *Example City* with  $N$  inhabitants a number of  $n_{\text{ICU}} = 40$  (rounded to the next integer) ICU beds. As tolerance we choose  $\xi = 0.1$  and we recall that  $\varphi^+ = (1 + \xi)n_{\text{ICU}}$  is the threshold that the number  $I_S$  of symptomatic infected should not exceed, cf. (2.4). For purposes of comparison, Fig. 5.1 shows the simulation results in the case that the policy makers take no action and hence  $u(t) = 0$  for all  $t \geq 0$ . It can clearly be seen that the number  $I_S(t)$  quickly increases above the available ICU capacity and the number of deaths rises dramatically; note that the effect of the exceeded ICU capacity is not considered in the model and hence the number of deaths might even be much higher.



(a) Susceptible, recovered and asymptomatic infected

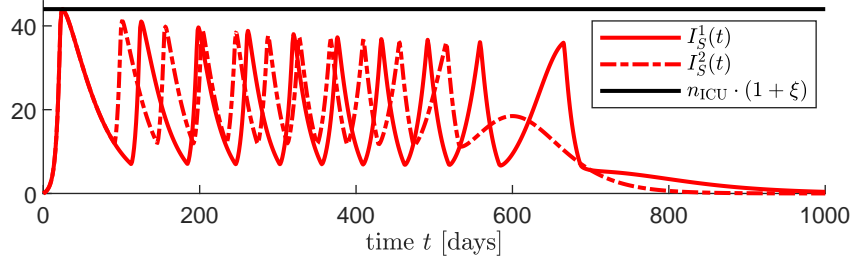
(b) Symptomatic infected and deceased

Fig. 5.1: Simulation of the epidemiological model (2.1) under  $u = 0$ .

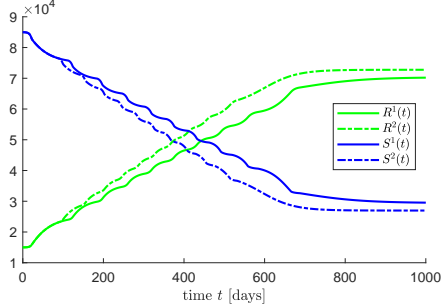
In contrast to this, Fig. 5.2 shows the same scenario but with social distancing measures enacted according to the control (3.1). For this simulation we have chosen  $\varepsilon^+ = 2\xi \cdot n_{\text{ICU}}$ , which is able to guarantee (2.4). Furthermore, we have chosen two different values for  $\varepsilon^-$ , namely  $\varepsilon_1^- = 1.75\xi \cdot n_{\text{ICU}}$  and  $\varepsilon_2^- = 3\xi \cdot n_{\text{ICU}}$ .

Similar to various studies before, the simulations depicted in Fig. 5.2 show that social distancing measures are capable of reducing the total number of infected individuals and, as a consequence, the total number of disease induced deaths. The feedback controller (3.1) is able to guarantee (2.4) as shown in Fig. 5.2(a). It can be seen that, while periods with  $u(t) = 1$  ensure that the ICU capacity is not exceeded, periods with  $u(t) = 0$  (no social distancing) result in quick increases of infection numbers and the switch in the controller (3.1) is triggered again after only a short period of time (at most a few weeks). This shows that lifting social distancing measures over a longer period of time will not be feasible until the end of the pandemic.

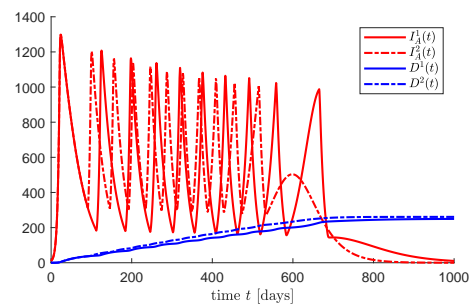
As shown in Fig. 5.2(d) the control input  $u_2$  corresponding to  $\varepsilon_2^-$  exhibits a faster switching pattern than the input  $u_1$  corresponding to  $\varepsilon_1^-$ . Several other simulations show that larger values of  $\varepsilon^-$  lead to a faster switching with shorter periods between the switches, but, on the other hand, the pandemic is defeated at an earlier time point (i.e., the time  $T > 0$  for which  $u(t) = 0$  for all  $t \geq T$  can be made smaller the larger  $\varepsilon^-$  is chosen). These are two conflicting objectives (few switches vs. shorter pandemic) and the policy makers



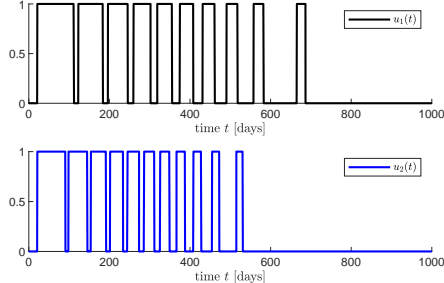
(a) Symptomatic infected and ICU capacity



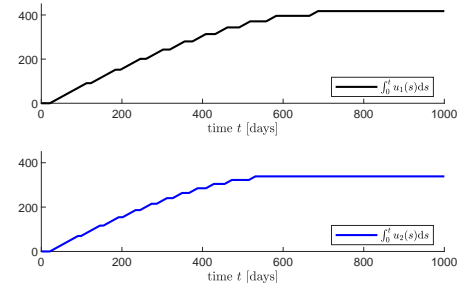
(b) Susceptible and recovered



(c) Asymptomatic infected and deceased



(d) Input functions



(e) Input costs

Fig. 5.2: Simulation of the epidemiological model (2.1) under control (3.1) with parameters  $\varepsilon_i^+$  and  $\varepsilon_i^-$  for  $i = 1, 2$ .

have to decide which should be favored; the controller design parameters may be adjusted accordingly.

Another observation reveals that the total number of deaths, i.e.,  $D_{\max} = \lim_{t \rightarrow \infty} D(t)$  depends on the choice of  $\varepsilon_i^-$ . Since minimizing  $D_{\max}$  seems a reasonable goal we have performed a set of simulations so that this is achieved, which led to the above value of  $\varepsilon_1^- = \varepsilon_2^-$ . As shown in Fig. 5.2(c) the number of deaths is indeed higher for  $\varepsilon_2^-$  and, as shown in Fig. 5.2(b), the total number of infected (represented by  $N - R(0) - S(t)$ ) is larger for  $\varepsilon_2^-$ .

Fig. 5.2(e) shows the input costs associated with the control signals  $u_1$  and  $u_2$  in terms of their  $L^1$ -norm on the interval  $[0, t]$  for  $t \geq 0$ . It can be seen that these costs are much higher for  $u_1$ . However, the “total costs” of the control strategy cannot be assessed by solely

considering the input costs, but the total duration of the pandemic and the total number of deaths (as mentioned above) must also be taken into account when defining a suitable total cost function – this is a topic of future research which should also involve objectives defined by policy makers.

Finally, by way of comparison, we like to note that effective control methods for the COVID-19 pandemic based on model-predictive control (MPC) have been developed in [9, 13]. However, MPC requires accurate model data and measurements of all state variables for feasibility. As shown in [9], uncertainty in the data and measurements can be compensated to a certain extent by using e.g. interval predictions, however it is not possible to prove *a priori* that MPC does not exceed the available ICU capacity. This is one of the advantages of the approach presented here.

**6. Conclusion.** We have presented a novel feedback controller which may serve as a decision making mechanism for policy makers during the COVID-19 pandemic. The controller is based on the bang-bang funnel controller from [11] and robust with respect to uncertainties in the parameters of the underlying epidemiological model. It only requires the measurement of the number of individuals with moderate to severe symptoms, and it is able to keep this number below a threshold determined by the ICU capacity at any time.

Simulations illustrate that the proposed controller (3.1) is able to achieve the control objective and that a relaxation of social distancing policies may quickly lead to increasing infection numbers. Although a relaxation of the distancing measures over a period of only 1–2 weeks may seem pointless, the simulations suggest that a temporary increase of infection numbers, while preventing that the ICU capacity is exceeded, ensures a less extended time course of the COVID-19 pandemic compared to a strict lockdown. At the same time this allows a resumption of social and economic activities during these periods. By a continuous improvement of the available data and the simulations it should be possible to obtain better forecasts of when the input signal switches, which would allow the people to prepare for possible measures or relaxation.

Although the results presented in this work are quite promising regarding automated signals for social distancing measures, this is only a first step towards a universal technique. Future research needs to focus on methods which incorporate different levels of social distancing measures compared to only the two levels (full measures or no measures at all) considered in the present paper. A balanced use of such regulations is more practicable and will be accepted by a wider public. Typical examples are cancelation of big events, carrying face masks in supermarkets and public transport or working from home when possible; these measures may be included in the model by additional control values  $u_i \in (0, 1)$  as suggested e.g. in [9].

Another topic of future research is the combination of different models for different countries or regions, where different control values (due to government policies) are active. In particular, it needs to be investigated how the interactions between different regions, based on migration flows, influence the spread of the disease. Such an approach will possibly reveal which social distancing measures must be taken in neighboring regions with different outbreak levels.

Last but not least, we like to note that the approach presented here is not restricted to the model (2.1), but the feedback controller (3.1) can be applied, *mutatis mutandis*, to any epidemiological model available in the literature, appended by the dynamics for the population response.

## REFERENCES

- [1] A. D. AMES, T. G. MOLNÁR, A. W. SINGLETARY, AND G. OROSZ, *Safety-critical control of active interventions for COVID-19 mitigation*, IEEE Access, 8 (2020), pp. 188454–188474.
- [2] T. BERGER, S. OTTO, T. REIS, AND R. SEIFRIED, *Combined open-loop and funnel control for un-*

*deractuated multibody systems*, Nonlinear Dynamics, 95 (2019), pp. 1977–1998.

[3] T. BERGER AND A.-L. RAUERT, *Funnel cruise control*, Automatica, 119 (2020), p. Article 109061.

[4] T. BERGER AND T. REIS, *Zero dynamics and funnel control for linear electrical circuits*, J. Franklin Inst., 351 (2014), pp. 5099–5132.

[5] S. GRUNDEL, S. HEYDER, T. HOTZ, T. K. S. RITSCHEL, P. SAUERTEIG, AND K. WORTHMANN, *How much testing and social distancing is required to control COVID-19? some insight based on an age-differentiated compartmental model*. Preprint available at <https://arxiv.org/abs/2011.01282>, 2020.

[6] C. M. HACKL, *Non-identifier Based Adaptive Control in Mechatronics—Theory and Application*, vol. 466 of Lecture Notes in Control and Information Sciences, Springer-Verlag, Cham, Switzerland, 2017.

[7] A. ILCHMANN AND S. TRENN, *Input constrained funnel control with applications to chemical reactor models*, Syst. Control Lett., 53 (2004), pp. 361–375.

[8] S. KISSLER, C. TEDIJANTO, M. LIPSITCH, AND Y. H. GRAD, *Social distancing strategies for curbing the COVID-19 epidemic*. medRxiv preprint, <http://dx.doi.org/10.1101/2020.03.22.20041079>, 2020.

[9] J. KÖHLER, L. SCHWENKEL, A. KOCH, J. BERBERICH, P. PAULI, AND F. ALLGÖWER, *Robust and optimal predictive control of the COVID-19 outbreak*, Annu. Rev. Control, (2020). In Press, doi: 10.1016/j.arcontrol.2020.11.002.

[10] D. LIBERZON AND S. TRENN, *The bang-bang funnel controller (long version)*. preprint available from the websites of the authors, 2010.

[11] ———, *The bang-bang funnel controller for uncertain nonlinear systems with arbitrary relative degree*, IEEE Trans. Autom. Control, 58 (2013), pp. 3126–3141.

[12] B. F. MAIER AND D. BROCKMANN, *Effective containment explains subexponential growth in recent confirmed COVID-19 cases in China*, Science, 368 (2020), pp. 742–746.

[13] M. M. MORATO, S. B. BASTOS, D. O. CAJUEIRO, AND J. E. NORMEY-RICO, *An optimal predictive control strategy for COVID-19 (SARS-CoV-2) social distancing policies in Brazil*. Preprint available at <https://arxiv.org/abs/2005.10797>, 2020.

[14] F. PIGUILLEM AND L. SHI, *The optimal COVID-19 quarantine and testing policies*. Technical Report, Einaudi Institute for Economics and Finance, EIEF Working Paper 20/04, 2020.

[15] A. SENFIELDS AND A. PAUGURS, *Electrical drive DC link power flow control with adaptive approach*, in Proc. 55th Int. Sci. Conf. Power Electr. Engg. Riga Techn. Univ., Riga, Latvia, 2014, pp. 30–33.

[16] H. STREECK ET AL., *Infection fatality rate of SARS-CoV-2 infection in a German community with a super-spreading event*. medRxiv preprint, <http://dx.doi.org/10.1101/2020.05.04.20090076>, 2020.